IJISET - International Journal of Innovative Science, Engineering & Technology, Vol. 1 Issue 8, October 2014.

www.ijiset.com

ISSN 2348 – 7968

Performance Analyses of a Simple Digital Nuclear Radiation Measurement System for Gamma Ray Spectroscopy

Onyemaechi N. Ofodile[1], Matthew N. Agu[2]

[1]Manpower Training and Capacity Development Directorate, Nigeria Atomic Energy Commission, Abuja, Nigeria,

[2]Nuclear Power Plant Development Directorate, Nigeria Atomic Energy Commission, Abuja, Nigeria

Abstract

There are 3 errors that are associated with the measurement of nuclear radiations. These are from the noise accompanying an incident radiation pulse, the dead time required for the processing of the incident radiation pulse and the pile-up of pulses. In analogue processing, these errors are often downplayed leading to the obtained results not being as accurate as they should be. Available digital processors can solve these problems to a large extent but their complex natures and high costs make it difficult for most university laboratories to easily acquire them for laboratory experiments. We have designed and implemented a digital nuclear processing system that will significantly solve the 3 problems associated with nuclear radiation pulse processing as well as being less complex and cheap. The analyses of the implemented digital nuclear radiation processing system (DNRPS) showed that the system has progressively more superior energy resolution than a popular analogue system based on the *Integrated Computer Spectrometer – Peripheral Connect Interface* (ICS-PCI) set up at high gamma energies of above 1000 KeV. In terms of activity of sources, the DNRPS provides more accurate values than the ICS-PCI setup at all gamma energies from 511 KeV to 1332 KeV.

Keywords*: Dead Time, Digital Processing, Energy Resolution, Net Count, Peak Detection, Pile-up Detection, Spectroscopy*

1. Introduction

Analogue and digital electronics means are used in the processing of nuclear radiations to determine the type, energy and intensity of such radiations. The processing is adversely affected by the responses of the electronic devices or components which culminate in 3 kinds of errors, namely, noise associated with a detected radiation and its processing, dead time and pile-up losses. Dead time loss arises due to the time interval required to process a radiation pulse during which another detected radiation pulse cannot be processed. Pile-up loss arises due to the fact that two radiation pulses may arrive close to themselves in time with the result that their values overlap and are summed up such that the new summed value does not represent any of the two pulses. This constitutes serious distortions to the accuracy of measured pulse values.

Many nuclear/radiation physics laboratories still use gamma ray spectroscopy systems that employ analogue schemes to implement the processing of radiation pulses while digital schemes are used to interface the analogue processor to the computer. The effects of dead time and pileup errors are often down-played in these systems, leading to serious errors in the observed results. An alternative is the use of digital processing systems but the popularly available ones employ complex mathematical schemes such as adaptive trapezoidal/triangular filtering, symmetric or asymmetric cusp-like weighting and others. Such schemes require complex data operations such as digital multiplications, exponentiations, look-up tables for weighting functions, data set buffering for both time variant processing and inter-process synchronization in addition to complex dead time and pile-up error correction functions [1,2,3]. These are expensive to implement in terms of the processing times and costs of the required electronic components. In order to reduce these losses without compromising on the efficiency of the spectrometry, we have designed a relatively cheap, simple and much more accurate digital pileup inspection circuit [4] and a simple computer interface circuit [5] that can be used in a computer controlled gamma ray spectroscopy system for laboratory uses especially in developing countries. We have also derived an appropriate simple correction algorithm for the determination of accurate radiation counts [6].

ISSN 2348 – 7968

2. Description of the Digital Nuclear Radiation Measurement System

Fig. 1 shows the block diagram of the implemented digital nuclear radiation measurement system. The circuit blocks in the dashed box 1 constitute the main processing system which includes the filter, peak detection and pile-up inspection (FPPI) circuits such as in the progenitor of the more complex and expensive commercial products [2,3]. The Analogue Signal Conditioner (ASC) is contained in the dashed box 2 and includes the input amplifier stage and the Analogue-to-Digital Converter (ADC). It shapes and converts the incoming radiation pulses to appropriate digital forms for further digital processing. The computer interface circuit (CIC) interfaces the main processing section to the computer. The operations of the ASC, CIC and the FPPI are controlled by the computer through appropriate interface software.

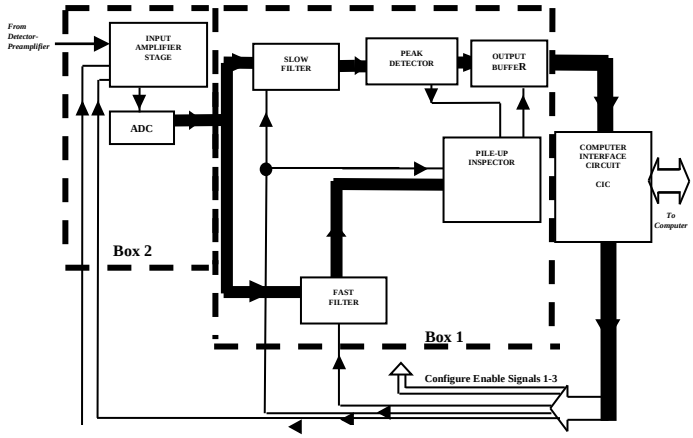

Fig. 1: Diagram of the Measurement System with the Component Blocks.

The FPPI comprises a slow channel triangular shaping filter, a fast channel triangular shaping filter, a peak detector, a pileup inspector and an output buffer. The peak value of the slow channel output constitutes a measurement of the energy of the corresponding detected radiation. The function of the pileup inspector is to ensure that the slow channel pulse outputs are sampled only when the captured peak values result from a good pulse event. A good pulse event is one which results from a pulse that is separated from both its predecessor and successor by a time interval that is at least greater than the slow channel's peaking time or pulse width. That is, a good pulse must be free of both leading edge and trailing edge pileups. Pileup inspection is implemented in such a manner that considers the only three possible conditions that could lead to pile-up situation. The interface software, dubbed "DNRPS" interfaces the DNRPS hardware to the computer and provides limited spectroscopic functions.

3. Data Analyses

3.1 Method

The approach adopted in the analyses of the implemented DNRPS is to compare the performance of the system with a popular gamma ray spectroscopy system such as the setup comprising a Teledyne Brown Type S-88-1 scintillator detector with a diameter of 2" or 5.08 cm, ORTEC 276 photomultiplier base with preamplifier and Spectrum ICS-PCI (MCA) hardware and software. The setup of the detector and photomultiplier base with preamplifier is used to determine the energy resolution and activities of several laboratory gamma sources using the Spectrum ICS-PCI (MCA) hardware and the implemented DNRPS hardware. The use of the common setup is to remove any biases in favour of one or the other system. The experimental setup of the DNRPS is as shown in Fig. 2.

The sources used were all of 1μCi activity at their manufacturing dates which give out gamma rays that cover the low energy 122 KeV and 136.47 KeV from ^{57}Co, the medium energy 511 KeV from ^{22}Na and 662 Kev from ^{137}Cs up to the high energy 1275 KeV from ^{22}Na, 1173 KeV and 1332 KeV from ^{60}Co.

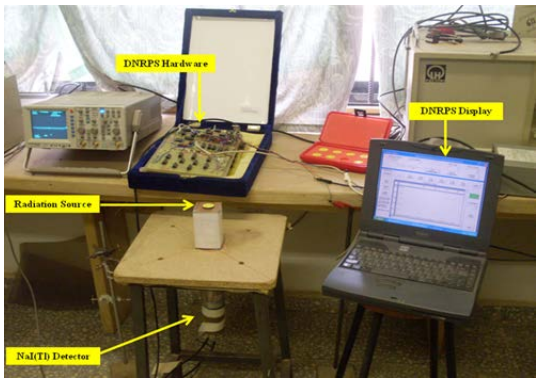

Fig. 2: Experimental Setup for the DNRPS

In all cases, the gamma sources were placed at a distance of 10.5 cm from the detector. In the case of ICS-PCI setup, a spectrum was accumulated for a live time (t) of 5 minutes. The sums under the photo peak in the forms of Gross and Net counts were recorded. Still retaining the gamma source U_1 as in the setup with ICS-PCI, the detector-preamplifier was connected to the DNRPS and a spectrum accumulated for a preset time of 5 minutes, equal to the live time (t) used in the case of the ICS-PCI system.

ISSN 2348 – 7968

3.2 Energy Resolution Theory

In theory, we expect gamma rays of a single energy to be recorded in one channel. In practice, each gamma ray appears as a peak, which can be approximated by a Gaussian function. The peak position corresponds to the energy of the gamma ray while the width of the Gaussian function gives us information on how precisely the detector and the pulse processing circuitries measure the energy of the gamma ray. The resolution of a spectrometer is therefore, a measure of its ability to resolve or differentiate between two peaks that are fairly close together in energy. The standard mathematical definition of energy resolution R in terms of gamma ray energy is given as [7]:

$$R = \frac{\delta E}{E} X 100\,\% \qquad (1)$$

where R is the resolution (in percent), δE is the full width of the peak at half the maximum count level (FWHM) measured in energy channels and E is the channel at the centroid of the photopeak.

3.3 Activities of Gamma Sources

The importance of accuracy in the measurement of activities of sources can be seen from the use of x-rays or gamma rays in radiation oncology which demands high precision and accuracy in the dose delivered to a tumour and its surrounding tissues. This is because the dose determines both the probability of cure and the possibility of radiation-induced complications. It has been reported that a realistic figure for the accuracy requirement of a prescribed dose to a target volume is 2 – 3 % [8]. To achieve this desired accuracy limit, sources of error in all the steps of radiation oncology must be identified and eliminated. A major source of error is the inaccurate instrument reading such as inaccurate radiation count rate which in turn leads to inaccurate determination of activity of a source and hence, inaccurate values of exposure rate.

At photon energies between 100 KeV and 2000 KeV (gamma energies of laboratory interest), the estimated exposure rate is related to the activity of a gamma source through [9]:

$$X = 6CEn \qquad (2)$$

where X is the exposure rate in R/hr, *C* is the activity in Curies, E is the energy of the radionuclide in MeV and *n* is the number of photons per disintegration.

In the laboratory, the NaI (Tl) detector can be used to measure the activities of radioactive sources. The activity measurement by an absolute method sustains many experimental uncertainties which must be kept under control in order to achieve a meaningful result. The main problems are that the source, detector and set-up dimensions are not accurately known. These include the exact distance of the source proper from the radiating surface of its housing and the detector's window thickness. Even for the detector intrinsic efficiency, data is not usually provided by the detectors' manufacturers, leaving the task to the potential user to compute it. The computed value is only an approximation and often times, far deviated from the realistic value.

From the experimental perspectives, the activity of a source U_1 is calculated from the formula:

$$\text{Activity of } U_1 = [(\Sigma U_1 - \Sigma_b)/t] \times 1/\varepsilon_p G B$$
$$= [(\Sigma U_1 - \Sigma_b)/t] \times P_{ds} \qquad (3)$$

where

ΣU_1 = sum under the photo-peak for the live time t

Σb = background for the same live time t

t = live time in seconds

ε_p = intrinsic peak efficiency for the gamma energy and detector size used

$$G = \text{Geometric Acceptance} = \frac{1}{2}\left(1 - \frac{d}{\sqrt{d^2 + a^2}}\right) \qquad (4)$$

d = source to detector distance in cm and

a = detector radius in cm

B = Branching Ratio which is the decay fraction of the unknown activity of source U_1. It is also the fraction of the total disintegrations in which the measured gamma is emitted or the fraction of the total disintegrations into the peak energy.

$$P_{ds} = 1/\varepsilon_p G B \qquad (5)$$

4. Results and Discussions

4.1 Energy Resolution

The energy resolutions obtained with the ICS-PCI and DNRPS setups are as shown in Tables 1

ISSN 2348 – 7968

and 2 respectively. It is observed that due to the single peak obtained from Co-57 source rather than two peaks at 122 KeV and 136.5 KeV, the resolution value of 22 % of the ICS-PCI setup is totally unreliable. At higher energy values, 1173 KeV, 1275 KeV and 1332 KeV, the DNRPS setup had better energy resolution and clearly outperformed the ICS- PCI as the gamma energy increased. However, it showed poorer energy resolution at energy values of 511 KeV (18.93 %) and 662 KeV (9.05 %) than the ICS-PCI setup, the poor performance being more at the lower energy value. The poor energy resolution of the DNRPS at low gamma energies is due mainly to the fact that at these low energies, the pulse values are equally low and usually swamped by noise of comparable values. Hence, any attempt to reduce the noise content also reduces the low pulse values. This problem can be solved through the use of a very low noise preamplifier module at the ASC frontend. Such preamplifiers are available but expensive.

Table 1: Determination of Energy Resolution for the ICS-PCI Setup

Energy (KeV)	Source	Centroid	FWHM	Resolution $R_{ICS\text{-}PCI} = \frac{\delta E}{E} X\,100\ \%$	Remarks
122	^{57}Co	81.01	17.82	22	NaI(Tl) detector has poor resolution at low gamma energies as it ages.
136.5	^{57}Co				
511	^{22}Na	332.95	31.25	9.39	
662	^{137}Cs	427.76	35.22	8.23	
1173	^{60}Co	740.14	39.52	5.34	
1275	^{22}Na	802.03	42.59	5.31	
1332	^{60}Co	834.99	39.32	4.71	

Table 2: Determination of Energy Resolution for the DNRPS Setup

Energy (KeV)	Source	ROI (channel)	Centroid (channels)	FWHM (channels)	Resolution $R_{DNRPS} = \frac{\delta E}{E} X\,100\ \%$	% Deviation $\Delta R = \frac{R_{ICS-PCI} - R_{DNRPS}}{R_{ICS-PCI}} \times 100\%$
122	^{57}Co	Unreliable single peak				
136.5	^{57}Co					
511	^{22}Na	73 - 95	84.5	76 – 92 (16)	18.93	- 101.60
662	^{137}Cs	100 -120	110.5	105 – 115 (10)	9.05	- 9.96
1173	^{60}Co	178 - 192	185.5	180 -189 (9)	4.85	+ 9.18
1275	^{22}Na	193 -207	200.5	196 – 205 (9)	4.49	+ 15.44
1332	^{60}Co	209 - 223	216.5	212 – 220 (8)	3.70	+ 21.44

The graphs of energy resolution versus energy shown in Fig. 3 for the two setups show that the two setups would have the same energy resolution of 6.5 % at gamma energy of about 980 KeV. The conclusion here is that for gamma energies below 950 KeV, the analogue setup such of the ICS-PCI has a better energy resolution. At gamma energies of 1000 KeV and above, the implemented DNRPS has a better energy resolution.

4.2 Activities of Sources

From the graph of energy against peak efficiency plotted for a detector-source distance of 10 cm shown in Fig. 4, the intrinsic peak efficiency ε_p of the used NaI (Tl) crystal (2" x 2" ie 5.08 cm x 5.08 cm) was determined for the various energies from Table 3 [10] and used in the determination of P_{ds} as shown in Table 4. Also the gamma branching ratios (B) [11] of the various energies and sources are used in the determination of P_{ds} while the activities of the various gamma sources as at the date of this experimentation were calculated and recorded in Table 5.

In the determination of the detector-source parameter P_{ds} of Table 4, the values of the intrinsic peak efficiency ε_p were obtained from a graph plotted with the values of the peak efficiency ε_p shown in Table 3.

Energy Range	Energy Value (KeV)	Gamma Source	ε_p	Branching Ratio B	Geometric Acceptance $G = \frac{1}{2}(1 - \frac{d}{\sqrt{d^2 + a^2}})$	$P_{ds} = 1/\varepsilon_p GB$
Low	122	^{57}Co	0.897	0.8560	0.0140	93.02630
						.50092
						.35622
						.32894
						.02882
						.23376
						.29763

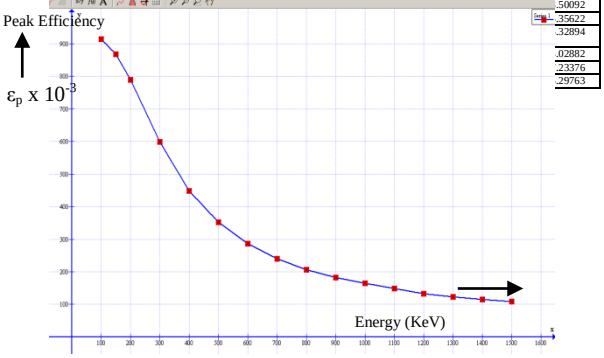

Fig. 4: Graph of Peak Efficiency Against Energy for a 2'' x 2'' NaI(Tl) Detector at a Source-Detector Distance of 10 cm Using the Values From Table 3.

Table 3: Peak Efficiency ε_p of the 2" x 2" [5.08 x 5.08 cm^2] NaI(Tl) Detector (Values were Generated Using GEANT3 Monte Carlo Code [10]

It is to be noted that the calculated P_{ds}

	Source-Detector Distance (cm)				Source-Detector Distance (cm)		
Energy (KeV)	3	10	30	Energy (KeV)	3	10	30
15	0.984	0.990	0.990	300	0.478	0.598	0.696
20	0.974	0.985	0.987	400	0.346	0.448	0.535
30	0.959	0.974	0.980	500	0.264	0.352	0.420
35	0.826	0.837	0.841	600	0.214	0.287	0.346
40	0.834	0.853	0.854	700	0.182	0.240	0.291
50	0.857	0.875	0.880	800	0.154	0.206	0.254
60	0.874	0.895	0.902	900	0.136	0.182	0.222
70	0.882	0.908	0.918	1000	0.121	0.164	0.202
80	0.886	0.913	0.928	1100	0.109	0.148	0.179
90	0.882	0.918	0.935	1200	0.098	0.133	0.165
100	0.875	0.914	0.936	1300	0.089	0.123	0.150
150	0.796	0.867	0.916	1400	0.084	0.115	0.139
200	0.683	0.789	0.867	1500	0.077	0.108	0.133

ISSN 2348 – 7968

Energy (KeV)	Source	ROI Sum Count	ICR_d	ROI Back-ground Count	Back-ground Rate ICR_b	Activity (μCi) = $\frac{P_{ds} \times (ICR_d - ICR_b)}{37{,}000\ (cps)}$	Deviation From Activity Value as at Date of Experiment
122	^{57}Co					A single peak was observed, hence, unreliable	
136.5	^{57}Co						
511	^{22}Na	62,767	211	5,145	17	0.6048	+ 3.66%
662	^{137}Cs	31,879	107	4,657	16	0.8001	+ 16.77%
1173	^{60}Co	15,585	52	3,430	11	0.5696	+ 29.13%
1275	^{22}Na	13,883	46	2,750	9	0.5672	+ 9.65%
1332	^{60}Co	12,798	43	2,217	7	0.5631	+ 29.94%

parameter values of Table 4 are not exact as the detector-source distance d = 10 cm could not be achieved exactly. The measured value of d was 10.5 cm. Furthermore, the exact distance of the source position in the source casing to the casing surface and the detector's window thickness are unknown and not taken into consideration of the detector-source distance. If these are known and taken into consideration, the value of G of Table 4 would have been smaller than that obtained.

Table 4: Determination of the Detector-Source Parameter Pds at a Distance d of 10.5 cm and Detector Radius a of 2.54 cm. Branching Ratios are from Table of Gamma Rays [11]

Gamma Source	Half Life $t_{1/2}$ (Days)	$\lambda = 0.6931/t_{1/2}$	Activity A_o on Date of Manufacture	Time (t) in days as at Date of Experiment	λ t	Activity A as at Date of Experiment (μCi)
^{57}Co	271.79	0.00255	1 μCi	607	1.54785	0.22170
^{22}Na	949.69	0.00072982	1 μCi	638	0.46562	0.62775
^{137}Cs	11205.5	0.00006185	1 μCi	638	0.03946	0.96131
^{60}Co	1924.06	0.00036	1 μCi	607	0.21852	0.80371

Table 5: Activities of Laboratory Gamma Sources as at Date of Experiments Using $A = A_o e^{-\lambda t}$

This would lead to an increase in the value of P_{ds} and hence, more accuracy in the calculations of activities in Tables 6 and 7. For example, if the gamma source is located midway in its casing, ie half-height of 0.95 cm and the detector's window thickness is 0.05 cm, then the source to detector distance would be 10.5 cm + 0.95 cm + 0.05 cm, ie, 11.5 cm instead of 10.5 cm used in the calculations of Table 4. The value of G would then be 0.01177 and not 0.0140.

Table 6: Practical Determination of Activities of Sources Using ICS-PCI Setup and NaI (Tl) Detector For a Live Time of 5 mins. (1 μCi = 37,000 cps).

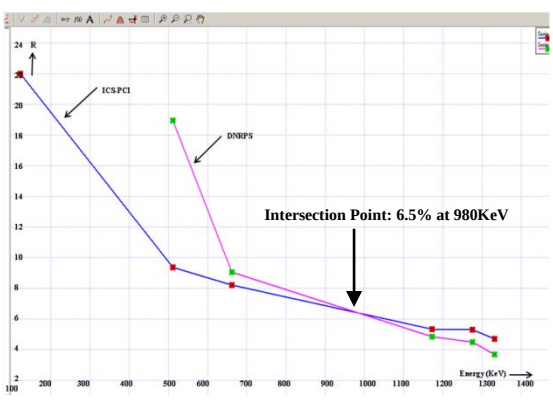

Fig. 3: Graph of Energy Resolution (R) Versus Energy (KeV)

Energy (KeV)	Source	Gross Count ΣU_G	Net Count ΣU_N	Activity (μCi) = $\frac{P_{ds} \times (\Sigma U_N)/t}{37{,}000\ (cps)}$	Deviation From Activity Value as at Date of Experiment
122	^{57}Co	141,366	105,503	A single peak was observed, hence, unreliable	
136.5	^{57}Co				
511	^{22}Na	87,538	69,217	0.7193	- 14.58%
662	^{137}Cs	32,683	23,568	0.6908	+28.14%
1173	^{60}Co	18,567	10,562	0.4891	+39.14%
1275	^{22}Na	15,631	10,828	0.5533	+11.86%
1332	^{60}Co	14,105	7,601	0.4076	+49.29%

Table 7: Practical Determination of Activities of Sources Using DNRPS Setup and NaI (Tl) Detector For a Preset Time of 5 mins. (1 μCi = 37,000 cps).

With the ICS-PCI setup, the Gross Count includes the background count and is the sum of all counts from all channels in the ROI. The Net Count is the sum of all counts from all channels in the ROI minus counts below the Compton edge line. The Net Count is therefore an approximation of the sum spectrum without background count. The Net Count is hence, used in the calculation of the activities of the sources as shown in Table 6. For the DNRPS, the counts and the input count rates were determined from the graphical and numerical displays as shown in Table 7.

For 511 KeV, the determined activity of Na-22 with ICS-PCI setup was 14.58 % higher than the calculated value while with the DNRPS setup, it was 3.66 % lower than the calculated value. It is clear that the activity determined with the DNRPS was more accurate. Also, though the gross counts obtained with the ICS-PCI were higher than those obtained with the DNRPS, for the other energies and sources, the activity values determined with the DNRPS were more accurate than those determined with ICS-PCI setup. While the deviations of the determined activities with both setups fall short of the 2 – 3% limit for radiation oncology accuracy, the values obtained with the DNRPS would obviously be preferred than those from ICS-PCI setup when applied to equation 2 for the estimation of exposure rates.

4.3 Quality of the Results

It is noted that the spectra with ICS-PCI setup did not take into account the noise and peak pile-up of pulses. Noise and pile up considerations with the ICS-PCI setup are downplayed. On the contrary, the noise and pile-up situations have been taken into account in the electronics of the DNRPS. The

ISSN 2348 – 7968

spectra and counts obtained with the DNRPS can therefore be said to be of higher quality than those obtained with the ICS-PCI. Furthermore, with the DNRPS, the application of the dead time and pile-up correction function will further improve the quality of the results leading to a more accurate determination of parameters such as the activity of sources.

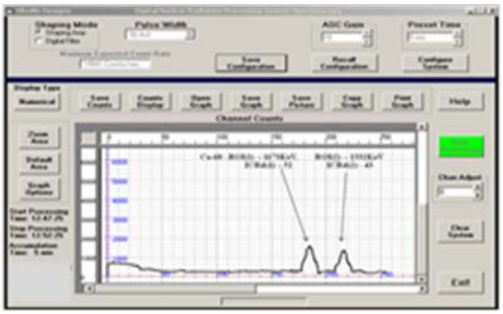

a: DNRPS Graphical Display for Co-60

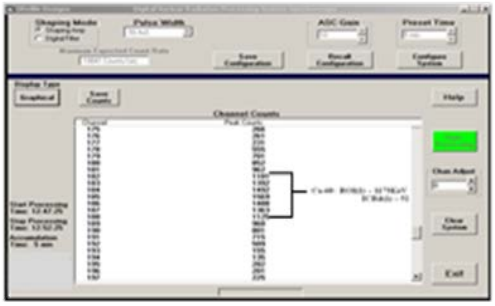

b: DNRPS Numerical Display for Co-60

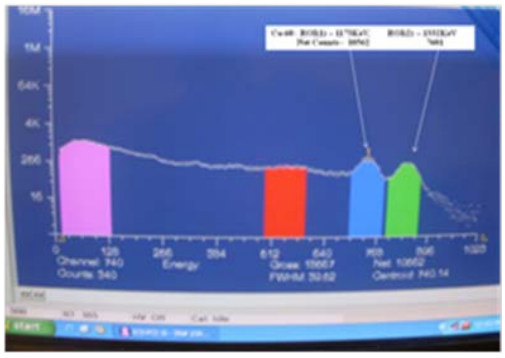

c: ICS-PCI Display for Co-60

Fig. 5: Snapshots of Spectra of Co-60 Source using both DNRPS and ICS-PCI Setups

In both cases of DNRPS and ICS-PCI, and for low energies of 122 KeV and 136.5 KeV, it was not possible to obtain any reliable spectrum. Infact, with the ICS-PCI setup, a single photo peak was obtained even with a very high background. The single peak was due to the inability of the detector to resolve these low and close energies into their respective peaks. Typical snapshots of the spectra from various sources using both DNRPS and ICS-PCI setups are shown in Figs 5 a-c for Co-60.

5. Conclusion

The performance analyses of the simple digital nuclear radiation measurement system through gamma ray spectroscopy experiments show that the system has superior energy resolution than the popular analogue system based on ICS-PCI setup at higher energies of 1173 KeV, 1275 KeV and 1332 KeV. However, it has poorer energy resolution at gamma energies of 511 KeV and 662 KeV than the ICS-PCI setup. From the determination of activity of sources, it is clear that the activity values obtained with the DNRPS were more accurate and therefore should be preferred than those determined with ICS-PCI setup.

It is noted that the spectra with ICS-PCI setup did not take into account the noise and peak pile-up of pulses as they are downplayed. On the contrary, the noise and pile-up situations have been taken into account in the electronics of the DNRPS. The spectra and counts obtained with the DNRPS can therefore be said to be of higher quality than those obtained with the ICS-PCI. Furthermore, with the DNRPS, the application of the dead time and pile-up correction function will further improve the quality of the results leading to a more accurate determination of parameters such as the activity of sources. The DNRPS has demonstrated a higher quality and accuracy of results when compared to a typical analogue setup such as with the ICS-PCI hardware and software.

References

[1] Mott, R.B. Digital pulse processor slope correction. US Patent No US2009/0033913 A1 of Feb 5, 2009. www.freepatentsonline.com.

[2] Warburton, W.K. and Zhiquing, Z., Method and apparatus for combinatorial logic signal processor in a digitally based high speed x-ray spectrometer. US Patent No 5873054 dated Feb 16, 1999. (www.freepatentsonline.com).

[3] www.xia.com/AppNotes/DXP_Pile.pdf: microDXPTechnical reference manual, version 1.0.3, May 16, 2006. X-ray Instrumentation Associates.

[4] Onyemaechi N. Ofodile, Matthew N. Agu, Novel Digital Pileup Inspection Circuit for a Gamma Ray Spectroscopy System. Journal of Nuclear and Particle Physics, 4(2), 2014: 58-64

ISSN 2348 – 7968

[5] Onyemaechi N. Ofodile, Matthew N. Agu, A Parallel 8-Bit Computer Interface Circuit And Software For A Digital Nuclear Spectroscopy System, Innovative Systems Design and Engineering Vol.5, No.2, 2014

[6] Agu, M.N. and Ofodile, O.N, Theoritical considerations in the design of dead time and pileup corrections in a simple two-channel digital nuclear radiation measurement system. International Journal of Applied Science and Technology 2(5), 2012, 130-136.

[7] G.F. Knoll, Radiation Detection and Measurement, J Wiley, New York, 1989, pages 96 to 102, pages 572 to 582, pages 607 to 609, page 669 and pages 673 to 677

[8] S.B Samat et al, Accurate Measurement of Exposure Rate From a 60Co Teletherapy Source: Deviations From the Inverse-Square Law, British Journal of Radiology, 73, 2000, pages 867 to 877

[9] Health Physics Society, Relationship Between Radionuclide Gamma Emission and Exposure Rate, http://www.hps.org/publicinformation/ate/faqs/

[10] Laboratorio de Instrumentacao E Fisica Experimental de Particulas, Lisboa, Portugal, Peak Efficiency ε_p Values of NaI(Tl) Detector. http://www.lip.pt/~luis/docs/Activity_Reports.pdf LIP/03-06 July 2003

[11] Korea Atomic Energy Research Institute, NDEL, Table of Gamma Rays, http://atom.kaeri.re.kr/gamrays.html.